

Fe(III)-MODIFIED MONTMORILLONITE AND BENTONITE: SYNTHESIS, CHEMICAL AND UV-VIS SPECTRAL CHARACTERIZATION, ARSENIC SORPTION, AND CATALYSIS OF OXIDATIVE DEHYDROGENATION OF PROPANE

T. GRYGAR^{1,*}, D. HRADIL¹, P. BEZDIČKA¹, B. DOUŠOVÁ², L. ČAPEK³ AND O. SCHNEEWEISS⁴

¹ Institute of Inorganic Chemistry ASCR, 250 68 Řež, Czech Republic

² Institute of Chemical Technology in Prague, Technická 5, 166 28 Prague 6, Czech Republic

³ University Pardubice, Cs. Legii 565, 532 10 Pardubice, Czech Republic

⁴ Institute of Physics of Materials ASCR, Žitkova 22, 616 62 Brno, Czech Republic

Abstract—Two major species were identified in Fe-treated montmorillonite: monomeric or dimeric hydroxoqua cations $\text{Fe}(\text{OH})_x^{(3-x)+}$ (form I), and polymeric structures with edge-shared $\text{Fe}(\text{O},\text{OH})_6$ (form II). These species have different electron spectra (absorption maximum is $29,600\text{ cm}^{-1}$ in form I, and $26,000$ and $28,000\text{ cm}^{-1}$ in form II), chemical and thermal stability, and electrochemical behavior. Form I behaves as a partly exchangeable cation in interaction with Cu^{2+} from Cu-trien solution and Ni^{2+} from Ni-EDTA, that can be used for selective quantitative analysis. On heating above the dehydration temperature ($\sim 100\text{--}150^\circ\text{C}$) montmorillonite with Fe^{3+} in form I is converted to a mica-like structure and Fe^{3+} ions are fixed more strongly in the montmorillonite structure. Form II behaves similarly to hydrous ferric oxides, but its thermal crystallization to hematite is postponed to $\sim 500\text{--}600^\circ\text{C}$. The Fe^{3+} cations in the interlayer space are much less thermally stable than Al pillars in pillared interlayered clays (PILCs). Form I is more active in oxidative dehydrogenation of propane, while form II is the active species in sorption of As and the non-specific combustion of propane. To produce only form II by the treatment of montmorillonite with Fe^{3+} , its load must be kept below $\sim 20\text{ wt.}\%$; otherwise the usual hydrous ferric oxides are formed.

Key Words—As sorption, Fe-montmorillonite, Fe-bentonite, Oxidative Dehydrogenation of Propane, Pillaring, Speciation of Fe.

INTRODUCTION

The modification of expandable clay minerals by Fe^{3+} has been much studied over the last decade in order to obtain so-called ‘pillared materials’, mostly for use as de-NOx catalysts (Chen *et al.*, 1995; Belver *et al.*, 2004a, 2004b) and as sorbents of As (Lenoble *et al.*, 2002; Izumi *et al.*, 2005). The Fe-pillared clay minerals were proposed as an analogy to Al-pillared minerals in the 1980s (Doff *et al.*, 1988). There has been insufficient characterization of the resulting materials with respect to the complexity of possible interactions between Fe^{3+} -hydrated ions and expandable clay minerals. The XRD patterns of some clay structures denoted as ‘Fe-pillared’ (Maes and Vansant 1995; Cañizares *et al.*, 1999; Lenoble *et al.*, 2002; Dramé, 2005) resemble those of highly disordered, delaminated structures such as the ‘house of cards’ as suggested by Chen *et al.* (1995). Repetition of syntheses did not always reproduce previous results, as stated explicitly by Maes and Vansant (1995). The extent of the replacement of the original interlayer cations has only rarely been checked (Izumi *et al.*, 2005), and an ionic occupation of the

interlayer space has not been examined by chemical means. The Fe-modified clays are sometimes characterized more by their porosity and materials properties and less by structural and chemical methods.

Pillaring of expandable clay minerals has systematically been studied using metal cations including Fe^{3+} (Zhao *et al.*, 1993; Chen *et al.*, 1995; Cañizares *et al.*, 1999; Lenoble *et al.*, 2002; Belver *et al.*, 2004a). However, the behavior of Fe^{3+} is very different and less understood than that of typical pillaring agents such as Al^{3+} . In those reports, Fe^{3+} ions in partly hydrolyzed Fe^{3+} solutions are commonly assumed to enter the interlayer space as nanosized particles or clusters to form nanostructured intercalated materials. Some authors found the interlayer basal spacing of Fe-pillared clay minerals to be $>20\text{ \AA}$ in calcined Fe-modified expandable clay minerals, *i.e.* $\sim 5\text{ \AA}$ greater than that of a two-layer hydrate of the expandable clay minerals (Cases *et al.*, 1997): this would indicate the incorporation of a polycation with a height of $\sim 10\text{ \AA}$, but such cations have not been isolated, unlike the Keggin cation built of $\text{Al}(\text{O},\text{OH})_6$ units. Some skepticism as to the ability of Fe ions to produce ordered pillared clay structures was expressed by Maes and Vansant (1995). The low thermal stability of Fe^{3+} -based pillars with respect to Al- and Al,Fe-pillars was established by Zhao *et al.* (1993) and Belver *et al.* (2004a) in spite of positive results reported by other authors (Cañizares *et al.*, 1999;

* E-mail address of corresponding author:

grygat@iic.cas.cz

DOI: 10.1346/CCMN.2007.0550206

Lenoble *et al.*, 2002). There is hence a need to understand better the behavior of Fe^{3+} interacting with clay minerals. One possible way in which to do this is an improvement of the product description. Electrochemical analytical methods (voltammetry of microparticles, VMP) and diffuse reflectance electron spectroscopy (DRS) were found suitable for Fe speciation in Fe-modified zeolites (Doménech *et al.*, 2002; Čapek *et al.*, 2005), though these methods have not been adequately exploited in analysis of Fe-modified clay structures.

The aims of this work were to re-evaluate the possibility of ‘pillaring’ montmorillonites by Fe^{3+} solutions in the absence of Al^{3+} and other metal ions prone to well defined oligomerization and to characterize the species present in Fe-treated montmorillonite. For speciation of Fe^{3+} , VMP, DRS and high-temperature powder X-ray diffraction (XRD) were used. An ion-exchange method with Ni-EDTA complex was developed that is similar to the Cu-trien ion-exchange method (Meier and Kahr, 1999) but the Ni-EDTA agent is able to exchange and solubilize non-polymerized Fe^{3+} from the interlayer space of the clay structure. All the analytical methods were used to understand the nature of Fe species in clay materials, tune the synthesis conditions, and identify the species active in sorption of As and catalysis of oxidative dehydrogenation of propane. In contrast to various Fe-modified zeolites, where high activity has been reported in oxidative dehydrogenation of propane with N_2O (Pérez-Ramírez and Gallardo-Llamas, 2005; Novoveská *et al.*, 2005), Fe-modified clay minerals have not yet been tested as catalysts in that reaction.

EXPERIMENTAL

Parent materials and Fe modification

Low-Fe montmorillonite type ‘Cheto’ SAZ-1 was received from The Clay Minerals Society Source Clays Repository (Purdue University, West Lafayette, Indiana). Its cation exchange capacity (CEC) is 120 meq/100 g and Ca and Na are the main interlayer cations, according to data provided by the supplier. Our estimate of the CEC, by Cu-trien, is 104 meq/100 g. The discrepancy may be due the fact that we used the montmorillonite sample in a naturally hydrated state, after handling under ambient laboratory conditions. Bentonite was obtained from a commercially exploited site, Hájek, in western Bohemia, Czech Republic (provided by Keramost Ltd). The bentonite from Hájek is reddish-brown material formed by alteration of basaltic tuffs developed in the first neo-volcanic stage of the Tertiary on the western slope of the Doupovské Mountains volcano. Analysis by XRD of the mean (whole-rock) specimen showed smectite as a major component, with a small admixture of micas, quartz, anatase and feldspar. The total Fe content in the specimen used in this work was 8.22% (chelatometric

titration). Free Fe oxides in the bentonite are below the detection limit of voltammetry of microparticles (~0.1–0.5%). Cu-trien exchange revealed that Ca and Mg are major interlayer cations in the smectite and the total CEC is 71 meq/100 g.

Chemical modification was performed in two ways. One, denoted as ‘Fe-modification’, involved a ~10 min interaction between parent material and $\text{Fe}(\text{NO}_3)_3 \cdot 9\text{H}_2\text{O}$ (Riedel-de Haën) in stirred aqueous suspension followed by filtration and washing in distilled water. The other, denoted as ‘Fe/OH-modification’, was performed with $\text{Fe}(\text{NO}_3)_3 \cdot 9\text{H}_2\text{O}$ solution after its forced partial hydrolysis by NaOH solution at a specified OH/Fe ratio varying from 0.7 to 3; in this case the interaction lasted from 1 h to 1 day. Two procedures were used to achieve the desired OH/Fe ratio; either the NaOH solution was mixed slowly with the $\text{Fe}(\text{NO}_3)_3 \cdot 9\text{H}_2\text{O}$ solution and stirred until clear solution was obtained, and then the parent material was added (OH/Fe ≤ 2), or NaOH was added slowly to a suspension of parent material in $\text{Fe}(\text{NO}_3)_3$ solution to prevent precipitation of free hydrous ferric oxides even at final OH/Fe ratio of >2. ‘Al-modification’ was performed by ~10 min of interaction of parent material with an aqueous solution of $\text{Al}(\text{NO}_3)_3 \cdot 9\text{H}_2\text{O}$.

Ferrihydrite was prepared by adding NaOH solution slowly to $\text{Fe}(\text{NO}_3)_3 \cdot 9\text{H}_2\text{O}$ solution to a final OH/Fe ratio of 3. The precipitate was filtered off, washed in distilled water and dried in air under ambient conditions.

Analytical methods

Diffuse reflectance spectra were acquired using a Perkin Elmer Lambda 35 spectrometer equipped with an integrating sphere (Labsphere) in 1 cm quartz cells. The reflectance was recalculated to Kubelka-Munk absorbance, and the positions of the absorption maxima were estimated from the minima of the 2nd derivative of 35 point FFT smoothed spectra (Scheinost *et al.*, 1998).

Voltammetry of microparticles (VMP) was performed with a μ Autolab device (Eco Chemie, The Netherlands) using a paraffin-impregnated carbon working electrode, Pt plate counter-electrode, and saturated calomel reference electrode (SCE). A $\text{CH}_3\text{COOH}-\text{CH}_3\text{COONa}$ buffer (1:1, total acetate 0.2 M) was used as a supporting electrolyte and linear sweep voltammetry from the open circuit potential towards negative potentials with a scan rate of 3 mV/s was deployed. The VMP signal is due to reduction of Fe^{3+} ions to Fe^{2+} possibly followed by dissolution of the species. The voltammetric peak potential (E_p) depends on the thermodynamic stability of the original Fe^{3+} species and the kinetics of its reduction and is evaluated by comparison with E_p of the reference compounds (Čapek *et al.*, 2005).

X-ray diffraction in a high-temperature chamber (HT-XRD) was performed using a HTK16 high-temperature chamber (Anton Paar), X’Pert PRO diffractometer and an X’Celerator multichannel detector (PANalytical). The

HT-XRD is based on monitoring the course of dehydration of interlayer cations of the expandable clay minerals (Grygar *et al.*, 2005).

^{57}Fe Mössbauer spectra were measured by a standard transmission method in a constant acceleration mode with a $^{57}\text{Co}(\text{Rh})$ radioactive source. The spectra were collected at 25 K using a closed He-cycle cryogenic system. A pure $\alpha\text{-Fe}$ foil was used as a calibration standard. The values of the isomer shift are related to $\alpha\text{-Fe}$ at room temperature. For computer processing of the spectra, a CONFIT package was used, yielding the values of the relative spectrum area, A , and values of the hyperfine parameters including hyperfine magnetic induction B_{hf} , isomer shift, δ , quadrupole splitting ΔE_{Q} , and quadrupole shift ε_{Q} (Žák, 1999).

Chemical analyses were performed using two selective cation-exchange agents. The Cu-trien method to estimate CEC was taken from Meier and Kahr (1999). Cu-trien solution was prepared from CuSO_4 and trien (trien = triethylenetetramine) to get the complex concentration 9 mM. A 100 mg sample was suspended in 10 mL of water; 5 mL of Cu-trien solution were added and the suspension was stirred for 10 min and then filtered to 50 mL flasks. The concentration of Cu^{2+} and alkaline and alkaline earth metal ions was analyzed by atomic absorption (AAS) or atomic emission spectroscopy (AES). Ni-EDTA (EDTA = ethylenediaminetetraacetate) solution was prepared from $\text{Ni}(\text{NO}_3)_2 \cdot 6\text{H}_2\text{O}$ and disodium salt of EDTA to get the complex concentration 50 mM. A 500 mg sample was suspended in 10 mL of water; 10 mL of the Ni-EDTA solution were added; the suspension was stirred for 90 min, filtered, and the Ni and Fe ions in the filtrate were determined by AAS. The total Fe in original and modified parent materials were determined by chelometric analysis after dissolution of the sample in a HF-HNO_3 mixture.

As sorption

The As^{V} solution, at a concentration of $\sim 2 \times 10^{-3}$ M (~ 150 ppm As), was prepared from $\text{NH}_4\text{H}_2\text{AsO}_4$ or KH_2AsO_4 of analytical-grade quality and distilled water. The As^{III} solution in the analogous concentration was prepared from NaAsO_2 of analytical-grade quality and distilled water. The model solution at initial pH value (≈ 5.5 for As^{V} and 8.8–9 for As^{III}) and the defined amount of sorbent was shaken in sealed polyethylene bottles at 20°C for 24 h. The product was filtered off; the filtrate was analyzed for residual As content by spectrophotometry using molybdenum blue with an absorption band at 825 nm (UNICAM 5625).

Catalytic tests

Oxidative dehydrogenation of propane was carried out in a glass through-flow micro-reactor at atmospheric pressure and at a temperature of 540°C, typically with 400 mg of the catalyst (0.25–0.50 mm) diluted with

2 cm³ of inert silicon carbide. A typical reaction mixture consisted of 5% C_3H_8 , 5% O_2 , and 10% N_2O in He; its flow was kept at 100 mL/min. Catalysts were pre-treated in an oxygen stream at 450°C for 1 h before each catalytic test. Gas chromatographic (CHROM 5, CZ) on-line analysis was carried out using a Porapak Q column, enabling separation of N_2O , CO_2 , hydrocarbons, alcohols and aromatics, and a 5 Å molecular sieve for analysis of N_2 and CO.

RESULTS

Ion exchange of Fe-treated montmorillonite with Ni-EDTA

The direct chemical analysis of the exchangeable cations should be the most straightforward method of analysis of modified clay minerals. One of the reasons why such analysis has not been done in any of the previous studies could be the hydrolytic instability of Fe^{3+} in aqueous solutions. For example, Fe-treated montmorillonite binds Cu^{2+} cations from Cu-trien solution, but almost no cations are evolved to solution. There is also a risk of chemisorption of Cu^{2+} on possible hydrous ferric oxide admixtures. The course of the ion exchange should be monitored by an agent replacing the Fe^{3+} ions in the interlayer space and simultaneously preventing the hydrolysis of Fe^{3+} ions evolved by the exchange. We hence treated the samples with a Ni-EDTA solution. A Ni^{2+} complex with EDTA is much less stable ($\text{pK} = 18.6$) than that of Fe^{3+} ($\text{pK} = 25.1$) (Meites, 1963), and Ni^{2+} has a similar affinity for the interlayer space as Cu^{2+} .

The course of interaction of Fe-treated montmorillonite (500 mg) with Ni-EDTA (20 mL 0.025 M Ni-EDTA) is shown in Figure 1; the concentration of Ni and Fe ions in solution reaches a steady state in ~ 1.5 h. The exchange experiments with Ni-EDTA were hence carried out using 500 mg of solid and 20 mL of 0.025 M solution of Ni-EDTA under stirring for

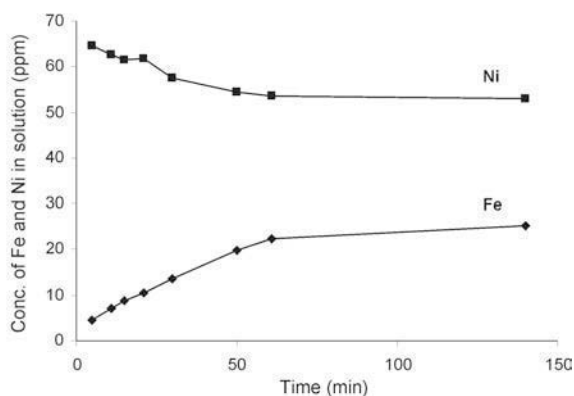


Figure 1. The evolution with time of Fe^{3+} and Ni^{2+} concentration in a suspension of a sample of Fe-treated montmorillonite in solution with Ni-EDTA.

90 min. The ion exchange is accompanied by a color change from blue (original Ni-EDTA) to green (Fe³⁺-EDTA complex is yellow). Then the suspension was filtered and the Ni and Fe ions in the filtrate were analyzed by AAS. In Figure 2 the final concentration of Fe³⁺ evolved by Ni-EDTA from series of Fe-treated montmorillonite samples is plotted against the decrease of total Ni²⁺, ΔNi^{2+} . The average molar ratio of Fe³⁺/ ΔNi^{2+} is equal to the slope of the line obtained by the least-squares method. We assume that the total charge of the exchangeable cations is preserved during the reaction. While Ni²⁺ is hydrolytically stable, Fe³⁺ ions in the interlayer space can be partly hydrolyzed (hydroxylated). During the cation exchange, Fe³⁺ cations evolved to solution are bound in EDTA complex in solution and are hence stable towards hydrolysis and sorption. Under all these conditions, the Fe³⁺/ ΔNi^{2+} = 1.3 value, found experimentally (Figure 2), means that the formal charge of the Fe³⁺ species in the interlayer space of Fe-treated montmorillonite is ~1.5, *i.e.* its approximate formula can be written as [Fe(OH)_{1.5}(H₂O)_{4.5}]^{1.5+} if Fe³⁺ is in isolated octahedrons FeO₆ or [Fe₂(OH)₃(H₂O)₅]³⁺ if two FeO₆ octahedrons are merged by one joint edge.

The completeness of Ni-EDTA exchange was checked by comparison of the amount of Fe³⁺ evolved by Ni-EDTA treatment with the Fe content in the specimens obtained by the total chemical analysis after subtraction of Fe present in the original montmorillonite. The average efficiency of the Ni-EDTA extraction was 96% for nine specimens of Fe-treated montmorillonite examined. The selectivity of the Ni-EDTA treatment was checked using a sample of solid ferrihydrite under the same conditions of Ni-EDTA extraction. The aim was to estimate possible interferences by Ni²⁺ sorption on ferrihydrite and exclude the possibility that Ni-EDTA dissolves ferrihydrite. The total Ni²⁺ consumption, ΔNi^{2+} , by sorption, was 22.7 mmol/100 g and only 3.0 mmol per 100 g of dry ferrihydrite was evolved to

the solution, probably by a dissolution reaction. It is obvious that at least 87% of ΔNi^{2+} was consumed by sorption on the ferrihydrite surface and <0.3% ferrihydrite was dissolved (Fe_{TOT} in ferrihydrite is 52%). In the specimens with a hydrous ferric oxide admixture (see below), the Ni-EDTA method would be better evaluated from the Fe³⁺ evolved than from the ΔNi^{2+} value. In montmorillonite or bentonite samples treated with Fe³⁺/OH⁻ solutions, the Fe³⁺ so evolved was always less than the total Fe³⁺ added by the chemical modification.

Characterization of Fe-treated montmorillonite

The results of chemical analysis of Fe-treated montmorillonite are summarized in Table 1. The duration of interaction of ferric salt and montmorillonite was very short (~10 min) to minimize Fe³⁺ hydrolysis and to form Fe hydrated oxides, and the solid product was carefully washed by distilled water to remove traces of unbound Fe³⁺ ions. The maximal amount of Fe³⁺ so bound to montmorillonite SAZ-1 was ~55 mmol/100 g of montmorillonite. When the specimens with the maximum amount of exchanged Fe³⁺ were subjected to Cu-trien reaction, ~30 mmol of Cu²⁺/100 g of modified montmorillonite were consumed, while the parent montmorillonite treated by Cu-trien consumed 52 mmol of Cu²⁺/100 g of montmorillonite, *i.e.* Cu²⁺ was unable to replace all the Fe³⁺ ions from the interlayer space. The Cu²⁺ consumption of the partly Fe-exchanged montmorillonite increased with the decreasing Fe content, as the efficiency of the ion-exchange reaction increased. On the contrary, Ni-EDTA treatment of the samples evolved practically all chemically bound Fe³⁺ (the discrepancies were within the errors of analysis). The Fe³⁺ bound to montmorillonite from Fe(NO₃)₃ can hence be considered chemically very reactive, probably in a monomeric form. In Fe-saturated montmorillonite (Fe load in synthesis >75 mmol Fe/100 g of parent montmorillonite), very small amounts of the original exchangeable cations (Mg, Ca, Na) were found (Table 1), *i.e.* the interlayer space is practically completely occupied by Fe³⁺ species. Comparing the CEC of montmorillonite (52 mmol Cu²⁺/100 g) and the maximal amount of Fe³⁺ bound from ferric nitrate solution (60 mmol Fe/100 g), the formal charge of Fe in the interlayer space is ~1.7+. This value is similar to the formal charge estimated from the charge balance of Ni-EDTA exchange (1.5+) described above.

Electron spectra of Fe-treated montmorillonite (Figure 3) have the two strongest absorption bands of Fe³⁺-bearing species. The more intense band is centered at 29,600 cm⁻¹ and is obvious from the lowest concentrations of Fe³⁺, the weaker band is centered at 20,600 cm⁻¹. The heights of both of these absorption bands are linearly dependent on concentration (Figure 4), indicating a single Fe³⁺ species present in the entire series. The position of the band at

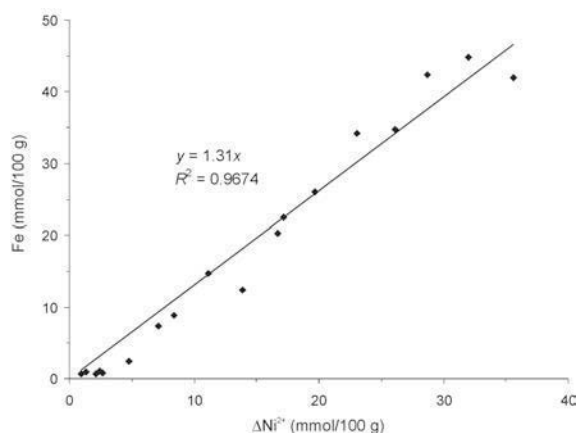


Figure 2. Ion exchange between Fe-modified montmorillonite and Ni-EDTA. The intercept was set as 0 in the regression line.

Table 1. Synthesis and properties of parent and Fe-treated montmorillonite SAz-1.

Fe load ¹ mmol/100 g	Synthesis		Product		Analysis by Cu-trien			Analysis by Ni-EDTA		
	Residual Fe in mother solution mg/L	Fe ³⁺ sorption efficiency ² %	Fe _{TOT} mmol/100 g	Fe _{TOT} -Fe _{parent} ³ mmol/100 g	ΔCu ²⁺ mmol/100 g	Ca ²⁺ mmol/100 g	Mg ²⁺ mmol/100 g	Na ⁺ mmol/100 g	ΔNi ²⁺ mmol/100 g	Fe ³⁺ mmol/100 g
0 (parent) ⁴				14.4		52			<1	<1
250	1168	17	55.7	41.4	30	0.4	0.9	0.1	35.6	42.0
100	320	43	57.2	42.8	32	1.5	1.2	0.2	32.0	44.8
75	156	63	61.6	47.2	31	1.4	1.1	0.5	28.7	42.4
50 ⁵	85	70	49.3	34.9	33	3.5	1.3	0.1	23.1	34.2
50 ⁵	129	54	41.3	27.0	35	4.0	1.8	0.1	17.2	22.4
50 ⁵	148	47	38.0	23.6					19.7	26.0
25	30	79	34.1	19.7	41	20.6	3.6	0.4	16.7	20.3
10	9	85	22.8	8.5	47	33.6	5.0	0.0	7.2	7.3
2.5	<1	98	17.3	2.9	49	39.8	5.3	0.1	4.8	2.5

¹ Load of Fe(NO₃)₃ per 100 g montmorillonite, ² percentage of Fe retained in the solid product, ³ difference between total Fe in modified montmorillonite and parent montmorillonite, ⁴ untreated montmorillonite SAz-1, ⁵ varying solid-to-liquid ratio in synthesis.

29,600 cm⁻¹ is very close to very weakly condensed Fe³⁺ ions in the Fe-modified zeolites (Čapek *et al.*, 2005) and to monomeric [Fe(OH)₂(H₂O)₄]⁺ and dimeric [Fe₂(OH)₂(H₂O)₈]⁴⁺ (Lopes *et al.*, 2002). The band at 20,600 cm⁻¹ can be assigned to a *d-d* electron-pair transition (EPT) of a structure with edge-sharing Fe(O,OH)₆ octahedra similar to that in FeOOH and ferrihydrite (Sherman, 1985; Scheinost *et al.*, 1998). However, in regular 3-D FeOOH structures, the EPT band is almost as strong as the near UV absorption; that is not the case in Fe-treated montmorillonite. The weak Vis absorption superimposed on stronger UV absorption is responsible for the pale yellow to light ochre-yellow color of the samples.

The assignment of the Fe(III) species to monomeric or very weakly condensed Fe structures is further proven by VMP and Mössbauer spectroscopy. Voltammetric peak potential, *E_p*, of the Fe-treated montmorillonite samples is +0.03 *V* vs. SCE (Figure 5), *i.e.* close to that of free (exchangeable) Fe³⁺ ions in Fe³⁺-treated zeolites (0 *V* vs. SCE, Čapek *et al.*, 2005). Mössbauer spectra of the Fe-treated montmorillonite (Fe_{TOT} = 2.3%) contain only a doublet of the magnetically non-interacting Fe³⁺ ions at both room temperature and 25 K (Table 4). At 25 K, even very poorly crystalline ferric oxides would be at least partly magnetically ordered (Cornell and Schwertmann, 2003).

On heating, the basal spacing of Fe-treated montmorillonite decreased and the mobility of the Fe³⁺ ions in both Cu-trien and Ni-EDTA exchange decreased continuously (Table 2). The basal spacings listed in Table 2 were obtained by conventional powder XRD with samples left in ambient laboratory conditions after heating. The results show that Fe³⁺ ions are fixed in the structure of montmorillonite, producing a mica-like structure which is not re-hydrated under ambient conditions. The position of the voltammetric peak of the Fe(III) species remained practically unchanged in the calcined samples, and only the absolute value of the current (the peak height) continuously decreased with increasing calcination temperature, as the chemical mobility of the species decreased.

Characterization of Fe/OH-treated montmorillonite

A solution of ferric nitrate partly neutralized by a drop-wise addition of NaOH up to the OH/Fe = 2 is commonly used for 'pillaring' clay materials (Cañizares *et al.*, 1999; Lenoble *et al.*, 2002; Belver *et al.*, 2004a; Izumi *et al.*, 2005). At this state of Fe³⁺ hydrolysis, the solution remains clear without precipitation. At a molar OH/Fe ratio of >2, ferrihydrite precipitation would be initiated, and so we added NaOH to the suspension of the parent material in ferric nitrate solution.

The synthesis conditions and characterization of specimens obtained by interaction of montmorillonite SAz-1 with partly hydrolyzed Fe(NO₃)₃ solution are summarized in Table 3. Only a minor fraction of total

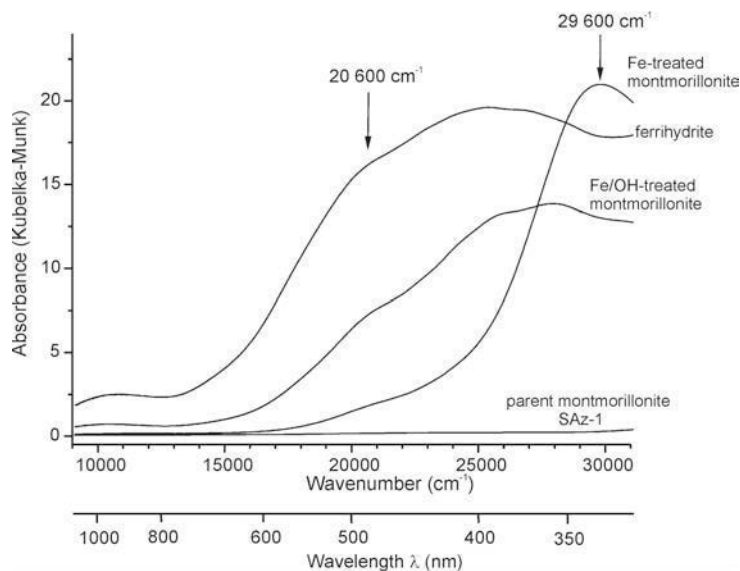


Figure 3. DRS pattern of parent montmorillonite, Fe-treated smectite, Fe/OH-treated montmorillonite and ferrihydrite. The diagnostic bands of individual species are indicated by arrows and the wavenumber of their absorption maximum.

Fe^{3+} used in synthesis was fixed in the solid product; the rest of the Fe^{3+} remained in solution and/or was removed by washing. In the specimens synthesized at $\text{OH}/\text{Fe} = 2$, practically all original exchangeable cations were

replaced by ferric ions; and up to 47 mmol/100 g were subsequently exchangeable by Ni-EDTA (corresponding roughly to 2.6% of the Fe^{3+} in the product). The majority of total Fe (~7%) is hence probably present outside the interlayer space. With the continuing hydrolysis of $\text{Fe}(\text{NO}_3)_3$ at $\text{OH}/\text{Fe} > 2$, the efficiency of the retention of Fe(III) in the solid product is growing, but some of the original exchangeable cations or even Na^+ from the NaOH additions remains in the interlayer space, and the content of Ni-EDTA-exchangeable Fe^{3+} decreases significantly. It is obvious, that at $\text{OH}/\text{Fe} > 2$, precipitation of hydrous ferric oxides is preferred to formation of interlayer Fe-species.

The color of Fe/OH-treated montmorillonite is reddish brown, much darker than in the case of Fe-treated montmorillonite, and accordingly the DRS patterns of these two materials are substantially different (Figure 3), indicating an increased degree of FeO_6 octahedra condensation. The spectrum of Fe/OH-treated montmorillonite resembles the spectrum of ferrihydrite more closely, as both have comparably strong absorption in Vis ($20,600 \text{ cm}^{-1}$) and in UV absorption, and UV absorption is shifted toward the Vis region, with two overlapped absorption maxima at $26,000$ and $28,000 \text{ cm}^{-1}$. The voltammetric peak potential is shifted to -0.13 V vs. SCE (Figure 5), similar to that for ferrihydrite (-0.15 V vs. SCE). In specimens with low OH/Fe ratio, two Fe^{3+} species with different electrochemical activity are present simultaneously, one at $+0.03 \text{ V vs. SCE}$ and the other at -0.15 V vs. SCE (Figure 5, sample with $\text{OH}/\text{Fe} = 0.7$), which indicates that the two VMP peaks belong to two distinct species and not to a continuous series of condensation products.

Mössbauer spectroscopy also confirmed certain condensation of Fe^{3+} ions in the Fe/OH-treated mont-

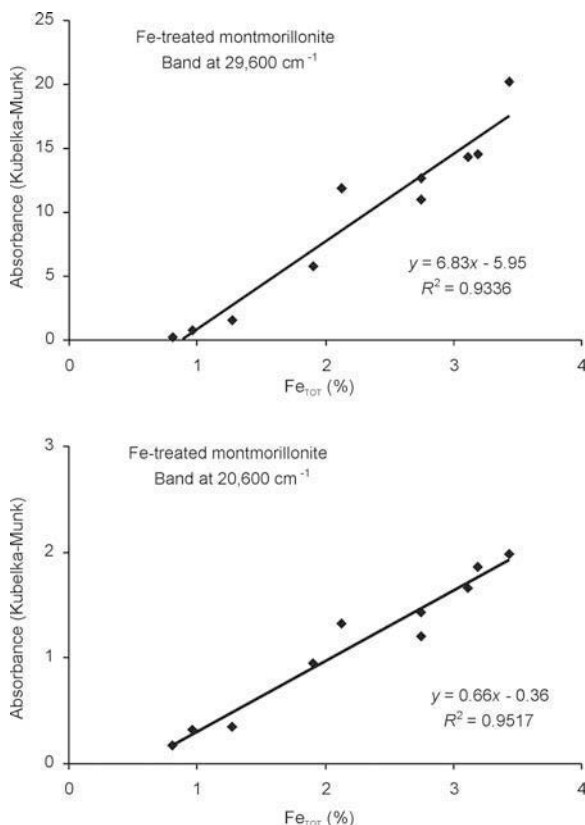


Figure 4. Concentration dependence of the absorbance of selected bands of Fe-treated montmorillonite.

Table 2. Properties of Fe-treated montmorillonite ($\text{Fe}_{\text{TOT}} = 50 \text{ mmol}/100 \text{ g}$) after its calcination. Basal spacing, d_{001} , was obtained by conventional powder XRD.

T ($^{\circ}\text{C}$)	d_{001} (\AA)	Analysis by Cu-trien		Analysis by Ni-EDTA	
		ΔCu^{2+} (mmol/100 g)		ΔNi^{2+} (mmol/100 g)	Fe^{3+} (mmol/100 g)
25	13.8	23		26	36
150	12.7	18		19	31
200	11.4	17		14	26
250	9.6	11		6	19
300	9.6	7		6	15
400	9.6	3		3	7
500	9.6	3		4	4
600	9.6	2		2	2

morillonites (Table 4). In a 25 K spectrum of sample obtained from solution with $\text{OH}/\text{Fe} = 0.7$, a sextet of magnetically ordered Fe^{3+} appeared beside a major doublet, while only the doublet is present in Fe-treated montmorillonite. The degree of magnetic ordering is, however, very low even in Fe/OH-treated montmorillonite; ferrihydrite would yield only sextets at a temperature of 25 K (Cornell and Schwertmann, 2003). The paramagnetic doublets in 25 K Mössbauer spectra in Table 4 are due to highly dispersed, very weakly condensed and disordered ferric oxidic structure. Accordingly, no definite XRD pattern of crystalline Fe^{3+} oxides was found in these specimens. The very low degree of ordering is also obvious from strongly hindered thermal crystallization of these Fe(III) oxide species to hematite in spite of a rather large total Fe^{3+} . The calcines of the Fe/OH-loaded montmorillonite were analyzed by XRD and VMP (Figure 6), and both methods identified hematite at calcination temperatures as high as 600°C at Fe load as high as 10% ($>170 \text{ mmol}/100 \text{ g}$), *i.e.* well above the value corresponding to CEC ($104 \text{ meq}/100 \text{ g}$).

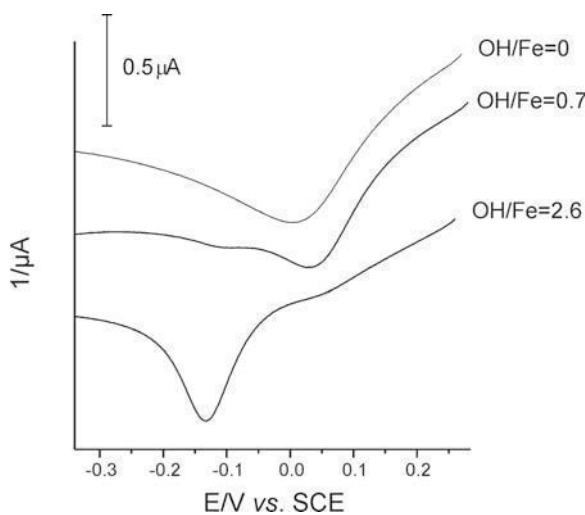


Figure 5. Voltammetric curves of individual ferric species in Fe- and Fe/OH-treated montmorillonite SAz-1. The curves are offset for clarity.

Sorption of As on Fe-treated montmorillonite and bentonite

Arsenic sorption is enhanced with increasing amounts of Fe in the modified clay mineral or bentonite (Table 5). The sorption capacity of the materials (in mmol/100 g) is $\sim 10\%$ of the total amount of Fe (in the same units) and is larger in Fe/OH-treated materials. The most efficient As sorbent listed in Table 5 is Fe/OH-modified bentonite, which had the greatest Fe/OH ratio (2.6) during synthesis and the largest final amount of Fe_{TOT} . This result is in agreement with the fact that pure free Fe(III) oxides are very efficient sorbents of As (Lenoble *et al.*, 2002; Izumi *et al.*, 2005) and with our observation that at $\text{OH}/\text{Fe} > 2$, hydrous ferric oxides are preferentially formed. The results summarized in Table 5 are in general agreement with the previously published data: As^{V} is sorbed better than As^{III} , and the sorption capacity achieved with the Fe/OH-treated bentonite at $c_{\text{As}} \approx 50 \text{ ppm}$, $Q \approx 0.3 \text{ mmol}/\text{g}$ ($22 \text{ mg As}/\text{g sorbent}$) is comparable with the results obtained with Fe-pillared clays and Fe oxides according

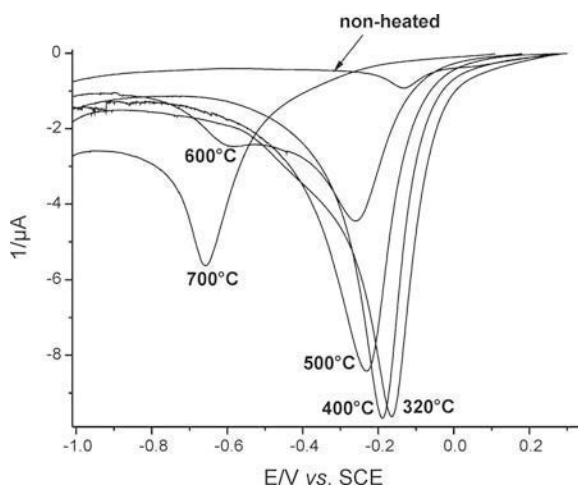


Figure 6. VMP study of the course of thermal crystallization of hematite in Fe/OH-treated SAz-1 ($\text{OH}/\text{Fe} = 3$, total $\text{Fe} = 17.2\%$). The hematite is responsible for the shoulder and (with its growing content) peak at about -0.6 V vs. SCE .

Table 3. Synthesis and properties of parent and Fe/OH-treated montmorillonite SAZ-1.

OH/Fe	Synthesis		Analysis		Analysis by Cu-trien		Analysis by Ni-EDTA		
	Fe load mmol/100 g	Duration ² h	Efficiency ³ %	Fe _{TOT} %	ΔCu ²⁺ mmol/100 g	Ca ²⁺ mmol/100 g	Na ⁺ mmol/100 g	ΔNi ²⁺ mmol/100 g	Fe ³⁺ mmol/100 g
0 (Parent)				0.8	52	<1	<1	0	<1
0.7	250	1	28	4.0	27	<1	<1	27	38
0.7	500	1	16	4.6	38	1	1	15	37
0.7	500	20	22	6.1	37	1	<1	26	37
1.5	217	12	53	6.4	30	1	1	30	47
2.0 ⁴	850	2	16	7.4	32	<1	1	26	46
2.0 ⁴	850	20	15	7.1	30	<1	<1	28	45
2.6	500	2	32	8.9	34	5	2	11	15
2.6	500	24	31	8.8	34	3	3	8	9
2.6	500	24	47	13.2	29	1	<1	14	12
3.0	500	1	62	17.2	32	16	16	16	7

¹ Load of Fe(NO₃)₃ per 100 g montmorillonite, ² duration of interaction of Fe/OH solution with the montmorillonite, ³ percentage of Fe bound to the solid product, ⁴ synthesis according to Lenoble *et al.* (2002)

Table 4. Mössbauer spectral parameters of Fe- and Fe/OH-treated montmorillonite obtained at 25 K.

Component	Area (%)	δ (mm/s)	ΔE _Q (mm/s)	B _{hf} (T)
Fe-treated montmorillonite, Fe _{TOT} = 2.3%				
D	99	0.35	0.37	
S	1	0.25	-0.04	27
Fe/OH-treated montmorillonite, OH/Fe = 0.7, Fe _{TOT} = 6.1%				
D	27	0.36	0.40	
S	20	0.34	-0.02	42
S	53	0.36	-0.04	25
Fe/OH-treated montmorillonite, OH/Fe = 2.6, Fe _{TOT} = 8.8%				
D	27	0.42	0.45	
D	22	0.55	0.31	
S	9	0.44	-0.01	43
S	42	0.54	0.00	26

Abbreviations: D – doublet, S – sextet, δ – isomer shift, ΔE_Q – quadrupole splitting, B_{hf} – hyperfine induction.

to Lenoble *et al.* (2002) and reported for Fe oxides by Garcia-Sanchez *et al.* (2002). Table 5 shows that the most efficient species at sorbing As is obviously the free hydrous Fe(III) oxide and not the interlayer Fe ions. Nevertheless, the presence of clay minerals in the sorbent is favorable, as it prevents Fe-oxide aggregation that would lead to a decrease in the specific surface area of the sorbent; a large specific surface area is required to achieve a large sorption capacity (Izumi *et al.*, 2005).

Table 5. Sorption of As on Fe-treated materials.

m/V (g L ⁻¹)	c _{RES} As ^V (mg L ⁻¹)	Q (mmol/g)	c _{RES} As ^{III} (mg L ⁻¹)	Q (mmol/g)
Fe-montmorillonite, Fe _{TOT} = 3.5%				
5	61	0.22	92	0.037
10	29	0.15	84	0.029
15	15	0.11	80	0.023
Fe/OH-montmorillonite, OH/Fe = 0.7, Fe _{TOT} = 4.6%				
5	46	0.26	71	0.093
10	19	0.17	65	0.055
15	8.9	0.13	46	0.054
Fe/OH-montmorillonite, OH/Fe = 1.5, Fe _{TOT} = 6.4%				
5	28	0.31	57	0.13
10	7.2	0.18	33	0.096
15	6.8	0.12	21	0.076
Fe/OH-bentonite, OH/Fe = 2.6, Fe _{TOT} = 13.3%				
5	37	0.30	54	0.26
10	3.0	0.19	15	0.18
15	0.4	0.13	0.7	0.13

m/V – sorbent-to-solution ratio, c_{RES} – residual concentration of As, Q – sorption capacity

Oxidative dehydrogenation of propane by Fe-treated montmorillonite and bentonite

Table 6 gives conversion of propane and selectivity of the formation of propene, CO and CO₂ in oxidative dehydrogenation (ODH) of propane. To achieve ~5–20% propane conversion, a temperature as high as 540°C was necessary. With one exception, all samples have much lower rates of conversion of propane in ODH by oxygen than by a mixture of O₂ and N₂O. This is in agreement with the results reported for Fe-modified zeolites. Nevertheless, it should be mentioned that the activity of Fe-modified clays have been much lower than that reported for Fe-modified zeolites. Pérez-Ramírez and Gallardo-Llamas (2005) reported ~25–50% conversion of propane, with selectivity to propene of ~40%. Novoveská *et al.* (2005) achieved ~20% conversion of propane with selectivity to propene of ~35% at 450°C using Fe zeolite as catalysts under the same composition of the gas phase.

While bentonite and Fe-treated montmorillonite promoted the formation of propene, Fe/OH-treated montmorillonite preferred non-selective combustion of propane and the intermediate propene to carbon oxides, mainly CO₂ (Table 6). This difference indicates that the two forms of Fe species in modified montmorillonites have substantially different catalytic behaviors. Surprisingly, the untreated bentonite has the best selectivity to propene formation and a relatively high degree of propane conversion compared to other materials. Hájek bentonite contains Fe mostly as a structural constituent because no free Fe(III) oxides were identified in this material up to the detection limit of VMP (0.1–0.5%). The Fe-treated montmorillonite was least active, consistent with our observation that under such a high temperature, the Fe³⁺ ions in Fe-treated

montmorillonite are fixed in the interlayer space of a mica-like structure and are hence inaccessible for the heterogeneous reaction. On the contrary, with increasing Fe_{TOT}, free ferric oxides are formed in Fe/OH-treated montmorillonite, and remain highly dispersed (non-crystalline) even at the relatively high operational temperature of the catalytic test.

DISCUSSION

Chen *et al.* (1995) estimated that only ~16% of the total Fe in pillared bentonite was present in the pillars, and the rest was bound in nanoparticulate Fe(III) oxides and other forms. To make the system even more complex, the diffraction patterns of the pillared clay minerals were not very clear, and sometimes even minor or ill-defined diffraction features at low angles were considered as proof of pillaring (Cañizares *et al.*, 1999; Lenoble *et al.*, 2002). The lack of certainty about homoionic Fe³⁺ pillars was first mentioned explicitly by Maes and Vansant (1995). Zhao *et al.* (1993) and Belver *et al.* (2004a) showed that Fe-pillared montmorillonite and saponite, respectively, collapse upon heating while Al₁₃ polycation-pillared structures are stable under the same conditions. In Figure 7 the thermal evolution of interlayer basal spacing of Al- and Fe-treated montmorillonite is shown. The collapse of the montmorillonite structure with hydrated interlayer cations to the mica-like structure occurs in both Fe/OH- and Fe-modified montmorillonite at much lower temperatures than in Al-modified montmorillonite, although non-polymerized Al³⁺ solution was used for modification of montmorillonite. None of the specimens described in this work has a thermal stability assigned to Fe-pillared clays in previous reports (Doff *et al.*, 1988; Cañizares *et al.*,

Table 6. Effect of Fe-treated montmorillonite on the course of oxidative dehydrogenation of propane. Reaction conditions are described in the Experimental section. Selectivity is expressed as the percentage of each component to the sum of products.

Oxidant	C ₃ H ₈ conversion (%)	Selectivity (% of products)			
		CO	CO ₂	C ₂ H ₄	C ₃ H ₆
Hájek bentonite, Fe _{TOT} = 8.2%					
O ₂	3.4	8	47	<1	44
O ₂ , N ₂ O	13.4	11	44	3	41
Fe-montmorillonite, Fe _{TOT} = 1.0%					
O ₂	2.2	<1	57	<1	43
O ₂ , N ₂ O	5.0	<1	50	<1	50
Fe-montmorillonite, Fe _{TOT} = 3.5%					
O ₂	10.7	25	48	<1	27
O ₂ , N ₂ O	9.3	21	46	<1	33
Fe/OH-montmorillonite, OH/Fe = 2, Fe _{TOT} = 4.9%					
O ₂	8.7	7	82	1	10
Fe/OH-montmorillonite, OH/Fe = 3, Fe _{TOT} = 17.2%					
O ₂	17.6	2	95	<1	3
O ₂ , N ₂ O	20.2	4	82	2	13

1999; Lenoble *et al.*, 2002; Belver *et al.*, 2004a; Dramé, 2005). All these facts indicate that it would be useful to identify directly the Fe species in Fe-modified clay minerals and to understand whether the pillaring is really the reason for their valuable materials properties.

The majority of Fe(III) in 'overloaded' clay materials is usually present in the form of free ferric oxides that causes crystallization of hematite on calcination at temperatures as low as 400°C (Zhao *et al.*, 1993; Chen *et al.*, 1995). The presence of α -FeOOH in the Fe/OH-treated clay minerals and free thermal crystallization of α -Fe₂O₃ on calcination at ~300°C (Dramé, 2005) mean that some of Fe-treated materials reported in the literature might merely be physical mixtures of clay minerals and free Fe(III) oxides. The materials obtained in this work do not contain the 'usual' Fe(III) oxides, as shown by their delayed thermal crystallization (Figure 6). Much care must hence be paid to careful speciation of Fe in the intercalated clay minerals, and to retain the highly dispersed nature of Fe(III) oxides in the Fe/OH-modified materials, the total Fe load must be kept below a certain limit. In the most common smectites, such as montmorillonite SAZ-1, the upper level of Fe load can be close to 20 wt.% Fe. Below this level, hematite is not formed even on calcination at 500°C. In Chen *et al.* (1995), montmorillonite with ~22% Fe_{TOT} was reported to produce traces of hematite by calcination already at 400°C.

The low degree of condensation of Fe(III) oxides in Fe/OH-treated montmorillonite is also demonstrated by Mössbauer spectroscopy (Table 4). Ferrihydrite, the least structurally ordered Fe(III) oxide, is magnetically ordered below 70–130 K (Cornell and Schwertmann, 2003), and hence at best about half of total Fe in Fe/OH-treated montmorillonite can be present in the form of particles of free ferrihydrite (sextets in Table 4).

The interaction between montmorillonite and Fe³⁺ in spontaneously (weakly) hydrolyzed ferric nitrate solu-

tion in pure distilled water proceeds easily as an ion exchange, as follows from the exchangeability of such Fe³⁺ ions by Ni-EDTA solution. This result is in line with the findings by Izumi *et al.* (2005). The Fe³⁺ ions in such Fe-exchanged montmorillonite can be substituted by Cu²⁺ from Cu-trien solution and Ni²⁺ from Ni-EDTA solution. The formal charge of exchangeable Fe³⁺ ion (estimated by an ion balance during the Ni-EDTA treatment and comparison of maximal load of the interlayer space with CEC of montmorillonite) is 1.5+ to 1.8+ per Fe ion. This partial effective charge is in reasonable agreement with monomeric dihydroxotetraqua-ferric complex cation [Fe(OH)₂(H₂O)₄]¹⁺ or binuclear bis(μ -hydroxo)octaaquadiferric complex cation [Fe₂(OH)₂(H₂O)₈]⁴⁺ (a formal charge 2+ per Fe) identified by DRS (according to reference data for dissolved complexes by Lopes *et al.*, 2002). The lack of extended polymerization of Fe(O,OH)₆ octahedra and the absence of ferrihydrite or other Fe(III) hydrated oxide is also proven by the results of voltammetry (Figure 5) and Mössbauer spectroscopy (Table 4). The small degree of Fe³⁺ condensation explains why the Fe-treated montmorillonite specimens are liable to collapse to a mica-like structure at temperatures as low as 200°C (Table 2, Figure 7). After heating at higher temperatures, the Fe³⁺-exchanged montmorillonite has lost its expandability and the Fe³⁺ ions are fixed in the clay structure.

CONCLUSIONS

Chemical, UV-Vis and Mössbauer spectral, X-ray diffraction, and electrochemical analyses revealed two major forms of Fe(III) in montmorillonite modified by ferric salt in aqueous solution: mono- or dimeric Fe³⁺ hydroxo-aqua-complex formed at lower pH (below precipitation of hydrous ferric oxides), and more polymerized Fe³⁺ oxide species formed by interaction of

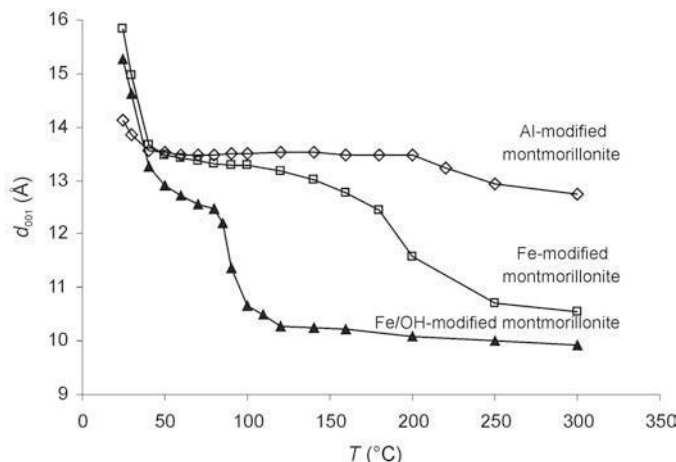


Figure 7. Thermal dependence of the basal spacing (001) of Fe-, Fe/OH- and Al-HT modified montmorillonite SAZ-1 obtained by HT-XRD.

montmorillonite with partly neutralized ferric salt especially at pH close to ferrihydrite formation. The genuine pillaring of montmorillonite by ferric species, comparable to the well established effect of the Al_{13} cation, has not been confirmed. The ferric species responsible for sorption of As and non-selective combustion of propane is the polymerized form, *i.e.* highly dispersed hydrous ferric oxide probably deposited on the external surface of clay mineral particles. It has a good stability for thermal crystallization to $\sim 500\text{--}600^\circ\text{C}$, when the original montmorillonite is collapsed to a mica-like structure. This conclusion is in agreement with the reports by Belver *et al.* (2004b, 2004c), according to which, Fe-impregnated inert supports such as alumina have similar catalytic activity in DeNO_x reaction to Fe,Al-pillared clays. Structural Fe in bentonite and mono- or dimeric Fe^{3+} cations are more selective in oxidative dehydrogenation of propane to propene.

ACKNOWLEDGMENTS

The work was supported by the Grant Agency of Czech Republic (202/04/0221), the Grant Agency of ASCR (IAA3032401), and Ministry of Education of the Czech Republic (MSM 0021627501). The authors also thank Michaela Hrušková for collecting the bentonite specimens, Jana Dörflová and Petr Vorm for sample preparation and chemical analysis, and Kamil Lang for providing DRS measurement facilities (all collaborators from Institute of Inorganic Chemistry ASCR).

REFERENCES

- Belver, C., Banares-Munoz, M.A. and Vicente, M.A. (2004a) Fe-saponite pillared and impregnated catalysts. I. Preparation and characterisation. *Applied Catalysis B – Environmental*, **50**, 101–112.
- Belver, C., Vicente, M.A., Martinez-Arias, A. and Fernandez-Garcia, M. (2004b) Fe-saponite pillared and impregnated catalysts II. Nature of the iron species active for the reduction of NO_x with propene. *Applied Catalysis B – Environmental*, **50**, 227–234.
- Belver, C., Vicente, M.A., Fernandez-Garcia, M. and Martinez-Arias, A. (2004c) Supported catalysts for DeNO(x) reaction based on iron clays. *Journal of Molecular Catalysis A – Chemical*, **219**, 309–313.
- Cañizares, P., Valverde, J.L., Sun Kou, M.R. and Molina, C.B. (1999) Synthesis and characterization of PILCs with single and mixed oxide pillars prepared from two different bentonites. A comparative study. *Microporous and Mesoporous Materials*, **29**, 267–281.
- Čapek, L., Kreibich, V., Dědeček, J., Grygar, T., Wichterlová, B., Sobalík, Z., Martens, J.A., Brosius, R. and Tokarová, V. (2005) Analysis of Fe species in zeolites by UV-VIS-NIR, IR spectra and voltammetry. Effect of preparation, Fe loading and zeolite type. *Microporous and Mesoporous Materials*, **80**, 279–289.
- Cases, J.M., Bérend, I., François, M., Uriot, J.P., Michot, L.J. and Thomas, F. (1997) Mechanism of adsorption and desorption of water vapor by homoionic montmorillonite: 3. Mg^{2+} , Ca^{2+} , Sr^{2+} , and Ba^{2+} exchanged forms. *Clays and Clay Minerals*, **45**, 8–22.
- Chen, J.P., Hausladen, M.C. and Yang, R.T. (1995) Delaminated Fe_2O_3 -pillared clay, its preparation, characterization, and activities for selective catalytic reduction of NO by NH_3 . *Journal of Catalysis*, **151**, 135–146.
- Cornell, R.M. and Schwertmann, U. (2003) *The Iron Oxides, Structure, Properties, Reactions, Occurrences and Uses*. Wiley-VCH, Weinheim, Germany, pp. 152–160.
- Doff, D.H., Gangas, N.H.J., Allan, J.E.M. and Coey, J.M.D. (1988) Preparation and characterization of iron oxide pillared montmorillonite. *Clay Minerals*, **23**, 367–377.
- Doménech, A., Pérez-Ramírez, J., Ribera, A., Kapteijn, F., Mul, G. and Moulijn, J.A. (2002) Characterization of iron species in ex-framework FeZSM-5 by electrochemical methods. *Catalysis Letters*, **78**, 303–312.
- Dramé, H. (2005) Cation exchange and pillaring of smectites by aqueous Fe nitrate solutions. *Clays and Clay Minerals*, **53**, 335–347.
- García-Sánchez, A., Alvarez-Ayuso, E. and Rodriguez-Martin, F. (2002) Sorption of As(V) by some oxyhydroxides and clay minerals. Application to its immobilization in two polluted mining soils. *Clay Minerals* **37**, 187–194.
- Grygar, T., Bezdička, P., Hradil, D., Hrušková, M., Novotná, K., Kadlec, J., Pruner, P. and Oberhänsli, H. (2005) Characterization of expandable clay minerals in Lake Baikal sediments by thermal dehydration and cation exchange. *Clays and Clay Minerals*, **53**, 389–400.
- Izumi, Y., Masih, D., Aika, K. and Seida, Y. (2005) Characterization of intercalated iron(III) nanoparticles and oxidative adsorption of arsenite on them monitored by X-ray absorption fine structure combined with fluorescence spectrometry. *Journal of Physical Chemistry B*, **109**, 3227–3232.
- Lenoble, V., Bouras, O., Deluchat, V., Serpaud, B. and Bollinger, J.C. (2002) Arsenic adsorption onto pillared clays and iron oxides. *Journal of Colloid and Interface Science*, **255**, 52–58.
- Lopes, L., de Laat, J. and Legube, B. (2002) Charge transfer of iron(III) monomeric and oligomeric aqua hydroxo complexes: Semiempirical investigation into photoactivity. *Inorganic Chemistry*, **41**, 2505–2517.
- Maes, N. and Vansant, E.F. (1995) Study of Fe_2O_3 -pillared clays synthesized using the trinuclear Fe(III)-acetato complex as pillaring precursor. *Microporous Materials*, **4**, 43–51.
- Meier, L.P. and Kahr, G. (1999) Determination of the cation exchange capacity (CEC) of clay minerals using the complexes of copper(II) ion with triethylenetetramine and tetraethylenepentamine. *Clays and Clay Minerals*, **47**, 386–388.
- Meites, L. (1963) *Handbook of Analytical Chemistry*. McGraw Hill Book Company, New York-Toronto-London, section 1, p. 45.
- Novoveská, K., Bulánek, R. and Wichterlová, B. (2005) Oxidation of propane with oxygen, nitrous oxide and oxygen/nitrous oxide mixture over Co- and Fe-zeolites. *Catalysis Today*, **100**, 315–319.
- Pérez-Ramírez, J. and Gallardo-Llamas, A. (2005) Impact of the preparation method and iron impurities in Fe-ZSM-5 zeolites for propylene production via oxidative dehydrogenation of propane with N_2O . *Applied Catalysis A: General*, **279**, 117–123.
- Scheinost, A.C., Chavernas, A., Barron, V. and Torrent J. (1998) Use and limitations of second-derivative diffuse reflectance spectroscopy in the visible to near-infrared range to identify and quantify Fe oxide minerals in soils. *Clays and Clay Minerals*, **46**, 528–536.
- Sherman, D.M. (1985) The electronic structures of Fe^{3+} coordination sites in iron oxides; Applications to spectra, bonding, and magnetism. *Physics and Chemistry of Minerals*, **12**, 161–175.
- Žák, T. (1999) CONFIT for Windows 95[®]. Pp. 385–390 in:

- Mössbauer Spectroscopy in Materials Science, Series III: High Technology* Vol. 66 (M. Miglierini and D. Petridis, editors). Kluwer Academic Publishers, Dordrecht, The Netherlands.
- Zhao, D.Y., Wang, G.J., Yang, Y.S., Guo, X.X., Wang, Q.B. and Ren, J.Y. (1993) Preparation and characterization of hydroxy-FeAl pillared clays. *Clays and Clay Minerals*, **41**, 317–327.
- (Received 3 May 2006; revised 31 October 2006; Ms. 1170; A.E. Peter Komadel)